

Synthesis of non-stoichiometric $\text{Bi}_2\text{O}_{4-x}$ by oxidative precipitation

A.S. Prakash^a, C. Shivakumara^a, M.S. Hegde^{a,*}, L. Dupont^b, J.-M. Tarascon^b

^a *Solid State and Structural Chemistry Unit, Indian Institute of Science, Bangalore 560012, India*

^b *Laboratoire de Réactivité et Chimie des Solides, Université de Picardie Jules Verne, Amiens, France*

Received 6 June 2006; received in revised form 11 July 2006; accepted 21 July 2006

Available online 11 September 2006

Abstract

$\text{Bi}_2\text{O}_{4-x}$, a Bi mixed-valence phase was prepared at 95 °C, by a precipitation process, in a basic medium with a highly oxidizing $\text{K}_2\text{S}_2\text{O}_8/\text{Na}_2\text{S}_2\text{O}_8$. This phase has a low thermal stability as it decomposes below 400 °C in a multiple step process by some O_2 losses prior to finally transforming into $\gamma\text{-Bi}_2\text{O}_3$. The as-prepared powders are 50–60 nm in size with a narrow size distribution. Optical spectra of $\text{Bi}_2\text{O}_{4-x}$ exhibit a broad absorption band with a band gap of ~ 1.4 eV as compared to 2.61 eV for Bi_2O_3 . The composition of this non-stoichiometric phase, which crystallizes in cubic fluorite related structure with a cell parameter of 5.538(3) Å, is $\text{Bi}_2\text{O}_{3.65 \pm 0.10}$.

© 2006 Elsevier Ltd. All rights reserved.

Keywords: A. Inorganic compounds; B. Chemical synthesis; C. X-ray diffraction; D. Optical properties

1. Introduction

The high-temperature modification of bismuth sesquioxide ($\delta\text{-Bi}_2\text{O}_3$), which crystallizes in the defect fluorite-type structure, is known as an excellent oxide-ion conductor [1]. Such a structure is usually stable over the 730–825 °C temperature [2], but it can be stabilized at room temperature by the substitution of various divalent, trivalent and pentavalent cations [1–4]. In the fluorite structure 1/4 of the oxide ion vacancies are accommodated in the lattice. Their arrangements, together with the stability of the ordered–disordered oxygen sublattice, depend upon the nature of the dopant cations and more specifically of their polarizability. Among the potential dopants to stabilize the fluorite structure of Bi_2O_3 , is Nb, W or Dy, which have the highest polarizability. In cubic $\text{Bi}_2\text{O}_{4-x}$, which was first reported by Jansen and Begemann [5], the fluorite phase is stabilized by the presence of some amount of Bi^{5+} in the structure. They have also reported the Bi_2O_4 and Bi_4O_7 with the monoclinic and triclinic pyrochlore-type structure, respectively. More specifically, the $\text{Bi}_2\text{O}_{4-x}$, whose structure was not detailed was prepared by the thermal decomposition of $\text{HBiO}_3 \cdot n\text{H}_2\text{O}$ and amorphous Bi_2O_5 under high oxygen pressures [5]. Although trivalent bismuth, Bi(III) is the most stable oxidation state for Bi in oxygen lattice, mixed Bi(III)/Bi(V) valences have been stabilized in some oxides such as BaBiO_3 [6], $\text{Ba}_{0.6}\text{K}_{0.4}\text{BiO}_3$ [7] and $\text{K}_{0.87}\text{Bi}_{1.13}\text{BiO}_3$ [8] with a few of them showing charge ordering and being superconductors. In these mixed-valence bismuth containing oxides, equivalent amount of Bi is oxidized to 5+ by substitution of divalent or monovalent ion for trivalent Bi ion. However, in binary oxides such as Bi_2O_4 , Bi_4O_7 , $\text{Bi}_2\text{O}_{4-x}$ [5,9,10] and in ternary oxides such as ZnBi_2O_6 and

* Corresponding author. Tel.: +91 80 2293 2614; fax: +91 80 2360 1310.

E-mail address: mshegde@sscu.iisc.ernet.in (M.S. Hegde).

MgBi_2O_6 [11], Bi(V) is stabilized regardless of the presence of mono or divalent ions in the structure. These materials are generally obtained using hydrothermal conditions rather than high temperature routes. Here we report the synthesis of the cubic fluorite $\text{Bi}_2\text{O}_{4-x}$ phase by an oxidative precipitation process, and we compared its chemical/physical properties with other Bi^{5+} containing binary oxides such as Bi_4O_7 and monoclinic Bi_2O_4 .

2. Experimental

In a typical preparation of $\text{Bi}_2\text{O}_{4-x}$, 22 g of NaOH (550 mmol) was dissolved in 500 ml of distilled water in a 1 l beaker and heated on a hot plate under constant stirring. When the basic solution temperature reached 95–100 °C, 16.35 g of $\text{K}_2\text{S}_2\text{O}_8$ (60.48 mmol) an aqueous solution of 10 g of $\text{Bi}(\text{NO}_3)_3 \cdot 5\text{H}_2\text{O}$ (20.61 mmol), dissolved in 1 ml of concentrated HNO_3 and 50 ml of distilled water, were added in that order. A brown precipitate instantaneously formed.

After 3 h of reaction time, the suspension was cooled down to room temperature and centrifuged at 4000 rpm for 10 min. The brown precipitate was washed with a weak electrolyte (1% NH_4NO_3) to avoid both its peptization and hydrolysis at neutral pH. The washing/centrifugation steps were repeated to ensure complete removal of soluble ions and finally the product was dried at 100 °C. We experienced that $\text{Na}_2\text{S}_2\text{O}_8$ can also be used as an oxidizer, instead of $\text{K}_2\text{S}_2\text{O}_8$, without any influence on the final product.

In addition, the Bi_2O_4 and Bi_4O_7 phases were prepared by hydrothermal synthesis following the procedures reported in the literature [9,10].

Powder X-ray diffraction pattern were recorded with a Philips diffractometer (PW 1710) with Cu $K\alpha$ radiation ($\lambda = 1.5418 \text{ \AA}$). Structural parameters were obtained using FullProf Refinement programme [12]. Transmission electron microscopy studies of samples were carried out with a Philips CM 12 transmission electron microscope operated at 100 kV. Optical absorption spectra were measured in UV, visible and near infrared regions with a Perkin-Elmer Lambda 35 spectrometer at 300 K. Thermogravimetric data were collected with a Mettler thermogravimetric analyzer at a heating rate of 5 °C/min under static air.

Chemical estimation of Bi and oxygen content were done with EDTA and iodometric titrations, respectively [13,14].

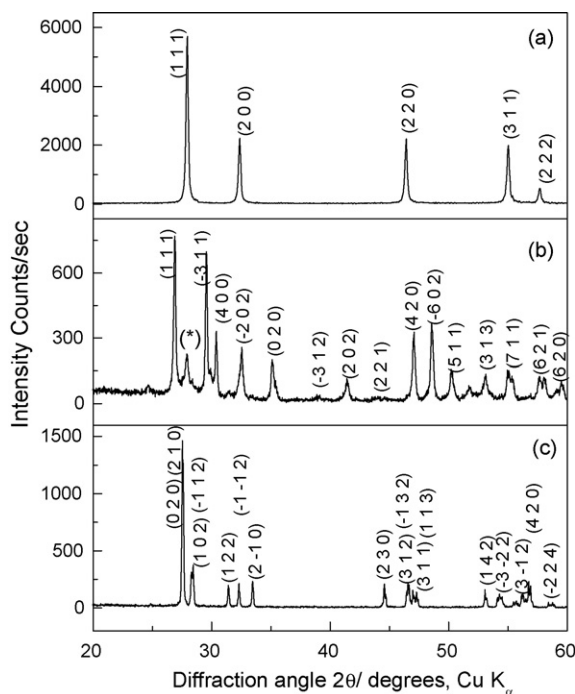


Fig. 1. X-ray diffraction patterns for different Bi-oxides: (a) cubic $\text{Bi}_2\text{O}_{4-x}$, (b) monoclinic Bi_2O_4 reflections from cubic $\text{Bi}_2\text{O}_{4-x}$, asterisk (*) impurity are indicated and (c) triclinic Bi_4O_7 .

Table 1
Lattice parameter, space group and crystal systems for Bi-oxides

Chemical formula	Crystal system, space group	Lattice constant		
		<i>a</i> (Å)	<i>b</i> (Å)	<i>c</i> (Å)
Bi ₂ O _{4–x}	Cubic, <i>Fm</i> 3 <i>m</i>	5.538(2)	5.538	5.538
Bi ₂ O ₄	Monoclinic, <i>C12/c1</i>	12.385(2)	5.121(7)	5.574(6)
Bi ₄ O ₇	Triclinic, <i>P</i>	11.421(8)	11.211(3)	10.788(2)
t-Bi ₂ O ₃	Tetragonal, <i>P-421c</i>	7.742(4)	7.742	5.631(6)
c-Bi ₂ O ₃	Cubic, <i>Pn</i> 3 <i>m</i>	5.529(2)	5.529	5.529
γ-Bi ₂ O ₃	Cubic, <i>I</i> 23	10.261(8)	10.261	10.261
δ-Bi ₂ O ₃ (PDF No: 01-074-1633)	Cubic, <i>Fm-3m</i>	5.665	5.665	5.665

3. Results and discussion

Bi-oxides with Bi in the 5+ oxidation state can be precipitated under highly oxidizing conditions by oxidizing agents such as K₂S₂O₈/Na₂S₂O₈, whose oxidation potential is higher than that required to oxidize Bi³⁺ to Bi⁵⁺ as indicated below:



Thus, the precipitation reaction of Bi₂O_{4–x} can be written as follows:

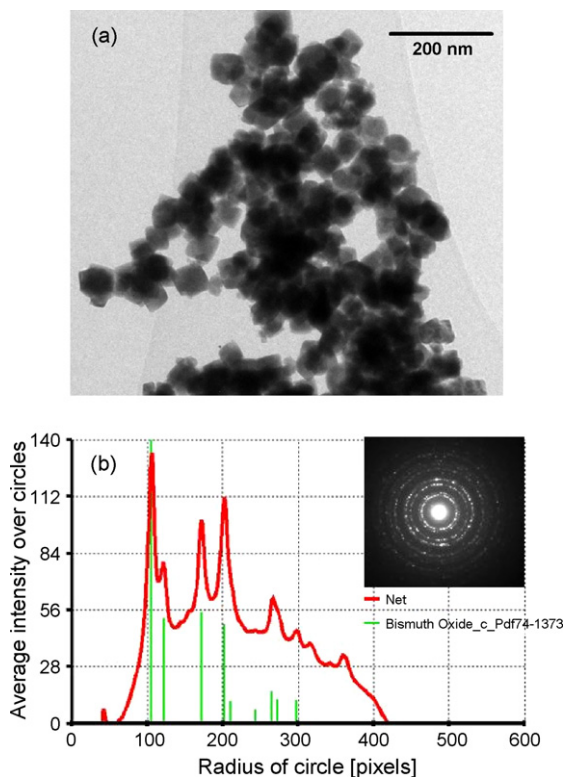
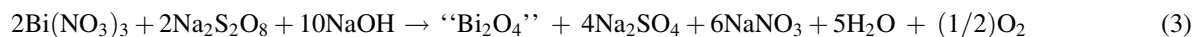


Fig. 2. Transmission electron micrographs of Bi₂O_{4–x}: (a) bright field image of 50–60 nm size particles and (b) process diffraction treatment of the SAED pattern shown in the inset.

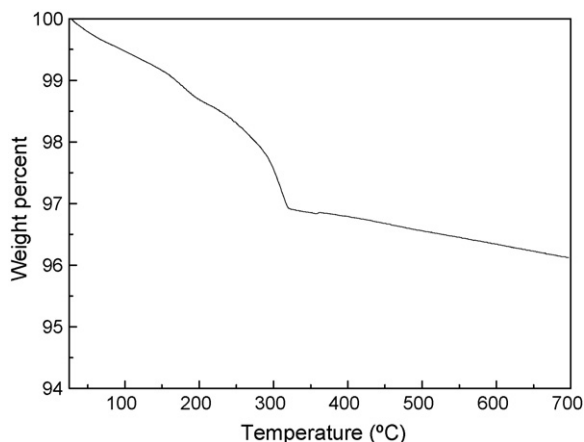


Fig. 3. Thermogravimetric analysis of $\text{Bi}_2\text{O}_{4-x}$ performed under flowing air.

The XRD pattern of the reddish brown powder obtained by precipitation ($\text{Bi}_2\text{O}_{4-x}$), together with that of monoclinic Bi_2O_4 and triclinic Bi_4O_7 , are shown in Fig. 1(a)–(c), respectively; the corresponding lattice parameters, which are in good agreement with the reported values [5,9,10], are given in Table 1.

A transmission electron micrograph of the as-prepared $\text{Bi}_2\text{O}_{4-x}$ is shown in Fig. 2(a). The particle sizes of as-prepared samples are in the range of 50–60 nm. The corresponding electron diffraction pattern (Fig. 2(b), inset) is composed of bright diffraction rings, and the corresponding X-ray pattern Fig. 2(b), calculated using process diffraction software [15], could be indexed with a cubic Bi_2O_3 cell (PDF No: 74-1373).

EDS analyses carried out on numerous crystallites did not show the presence of K or Na, despite the presence of a large quantity of alkali metal ions under the synthesis conditions. Thus neither potassium nor sodium is incorporated in the product.

Fig. 3 illustrates a TGA curve for “ Bi_2O_4 ” in air. The TG curve indicates multiple steps of weight loss due to oxygen removal. Oxygen evolution at these temperatures has been confirmed by temperature-programmed desorptions with Quadruple mass spectrometer. Corresponding X-ray diffraction pattern collected for the sample at various TG steps are presented in Fig. 4(a)–(c). The first 1.0% weight loss noted on the TGA trace was ascribed to absorbed water based on the absence of any changes in the XRD powder patterns. In contrast, the X-ray diffraction pattern collected after the second weight loss step (325 °C) in Fig. 4(b) showed a significant change. Careful analysis of the pattern indicated that it is composed of a mixture of metastable phases of Bi_2O_3 crystallizing in tetragonal

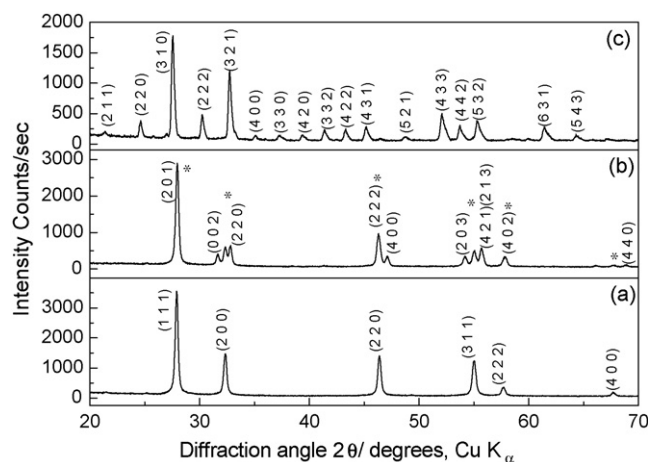


Fig. 4. X-Ray diffraction patterns of samples recorded at different Tg steps, showing phase transformations at various stages of decomposition. XRD patterns for (a) $\text{Bi}_2\text{O}_{4-x}$, (b) mixture of $\beta\text{-Bi}_2\text{O}_3$, and $\delta\text{-Bi}_2\text{O}_3$; the diffracted lines marked with an asterisk are due to $\delta\text{-Bi}_2\text{O}_3$ and (c) $\gamma\text{-Bi}_2\text{O}_3$.

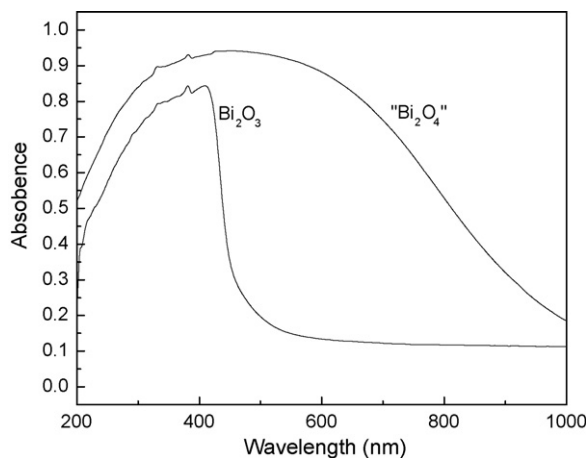


Fig. 5. Diffuse reflectance spectra for (a) $\text{Bi}_2\text{O}_{4-x}$ and (b) Bi_2O_3 .

($P-42_1c$) and cubic ($Pn3m$) structures which are denoted as $t\text{-Bi}_2\text{O}_3$ and $c\text{-Bi}_2\text{O}_3$. The Bragg peaks of the latter phase being marked by asterisk (Fig. 4b). The lattice parameters obtained for $t\text{-Bi}_2\text{O}_3$ and $c\text{-Bi}_2\text{O}_3$ are given in Table 1, and they are in good agreement with those reported (PDF No: 78-1793 and 74-1373).

The second weight loss step (2.12%) at 325 °C corresponds to the removal of 0.64 mol of oxygen from the parent Bi_2O_3 phase. Upon further heating from 325 to 700 °C, the TG profile indicates a small weight loss (0.8%), with the XRD of the 700 °C sample matching well with that of $\gamma\text{-Bi}_2\text{O}_3$ (Fig. 4(c)); its lattice parameter is in agreement with that reported (PDF No: 45-1344). From the thermogravimetric analysis, it can be deduced that the precipitated phase composition could be written as $\text{Bi}_2\text{O}_{3.64} \cdot 0.27\text{H}_2\text{O}$. Iodometric titrations showed an average oxidation state of 3.65 for Bi, which agrees well with the composition obtained from thermogravimetric analyses.

All of the as-prepared samples are dark brown, which is in agreement with other Bi^{5+} containing binary oxides such as Bi_4O_7 and Bi_2O_4 or ternary oxides such as in MgBi_2O_6 and ZnBi_2O_6 . We note from the diffuse reflectance spectra presented in Fig. 5 for $\text{Bi}_2\text{O}_{4-x}$ that the absorption edges of Bi^{5+} -containing samples shift to higher wavelengths leading to a band gap of ~ 1.4 eV as compared to 2.61 eV for $\gamma\text{-Bi}_2\text{O}_3$. For the latter, the band gap was ascribed to the electronic excitation from O (2p) to Bi^{3+} ($6p^0$) state [16]. In contrast, for $\text{Bi}_2\text{O}_{4-x}$, because part of Bi^{3+} gets oxidized to Bi^{5+} and the low lying Bi ($6s^0$) state is empty, it is tempting to ascribe the band gap to an O (2p)– Bi^{5+} ($6s^0$) electronic excitation.

Based on the initial crystal structure model for $\text{Bi}_2\text{O}_{4-x}$, the Rietveld refinement was carried out in the space group $Fm-3m$ considering a full Bi occupancy at 4a (0 0 0) site, and oxide ions distributed over 8c (1/4 1/4 1/4) sites. While the structural refinement was apparently satisfactory, the refinement of occupancy and thermal parameters of each ion were unusually large suggesting the possible existence of other sites. Moreover, careful examination of the intensities of the (2 2 0) and (3 1 1) reflections revealed these reflections were poorly fitted. The refinement with other model structures based on fluorite such as $\delta\text{-Bi}_2\text{O}_3$, Pr_7O_{12} , YUO_9 and $\text{In}_6\text{WO}_{12}$ were also not satisfactory. Finally, introduction of partial oxide ion occupancy at 4b (1/2 1/2 1/2) site in an ideal fluorite structure and redistribution of oxide ion occupancy among 4b and 8c sites gave a good fitting with acceptable values of occupation number and thermal parameters. The final refined parameters obtained for the above model are listed in Table 2. Both oxygen and Biso values converged and the relatively larger Biso values of oxygen suggest split oxygen occupancies in the lattice. Fig. 6 shows the observed, calculated and difference diffraction profile for $\text{Bi}_2\text{O}_{4-x}$. The refinement converged with

Table 2
Structural parameters obtained from Rietveld refinement for $\text{Bi}_2\text{O}_{4-x}$ phase

Composition	Space group	Lattice parameter, a	Atom	Position	x	y	z	Occupancy	Biso	R_{wp}
$\text{Bi}_2\text{O}_{4-x}$	$Fm3m$	5.538(2)	Bi(1)	4a	0.00	0.00	0.00	0.6538	0.0279	3.09
			O(1)	8c	0.250	0.250	0.250	0.6409	0.0847	
			O(2)	4b	0.500	0.500	0.500	0.01595	0.0847	

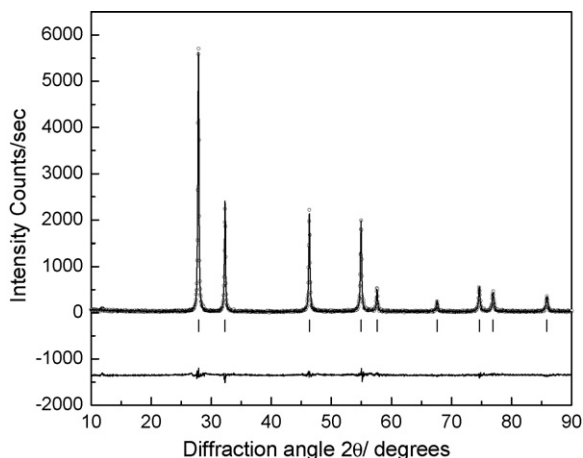


Fig. 6. Rietveld refined pattern for cubic $\text{Bi}_2\text{O}_{4-x}$; good fitting of experimental (\circ) with calculated (—) pattern, as well as the difference pattern (—) and Bragg positions ($|$).

$R_p = 2.99\%$, $R_{wp} = 3.09\%$, which are the lowest compared to the refinements with other models. The refined site occupancies with this model correspond to $\text{Bi}_2\text{O}_{3.96}$, which is near to the composition found from chemical analysis.

In $\delta\text{-Bi}_2\text{O}_3$, Bi^{3+} ions are located at 4a site and the oxide ions at 8c and 32f positions, whereas in cubic $\text{Bi}_2\text{O}_{4-x}$, Bi^{5+} and Bi^{3+} are randomly distributed at 4a sites and the oxide ions at 4b and 8c sites; thus the present compound is a disordered fluorite phase. The ionic radii of Bi^{5+} (0.76 Å) is smaller than that of Bi^{3+} (1.17 Å), and there is a decrease in the cell parameters of $\text{Bi}_2\text{O}_{4-x}$ ($a = 5.538(2)$ Å) compared to fluorite related cubic $\delta\text{-Bi}_2\text{O}_3$ ($a = 5.655$ Å) (PDF No: 74-1633), which crystallize in $Fm\text{-}3m$ space group [17]. Furthermore, the mean Bi–O bond distance in $\text{Bi}_2\text{O}_{4-x}$ is 2.57 Å, close to the bond distances of those found for $\text{Bi}^{3+}\text{-O}$ (2.56 Å) and $\text{Bi}^{5+}\text{-O}$ (2.10 Å) in monoclinic Bi_2O_4 [10].

4. Conclusions

We have reported for the first time the direct precipitation of $\text{Bi}_2\text{O}_{4-x}$ ($x = 0.36 \pm 0.10$) divided powders in aqueous medium with high yield. $\text{Bi}_2\text{O}_{4-x}$ crystallizes in $Fm\text{-}3m$ space group with cubic ‘a’ parameter of 5.538(2) Å. Cubic fluorite related structures are stabilized by some amount of Bi^{5+} , which upon thermal treatment is reduced to Bi^{3+} with release of O_2 to finally transform to $\gamma\text{-Bi}_2\text{O}_3$ above 400 °C. $\text{Bi}_2\text{O}_{4-x}$ exhibits a broad band gap of ~ 1.4 eV attributed to charge transfer of O (2p) to Bi^{5+} ($6s^0$) electrons.

References

- [1] N.M. Sammes, G.A. Tompsett, H. Näfe, F. Aldinger, J. Eur. Ceram. Soc. 19 (1999) 1801.
- [2] T. Takahashi, H. Iwahara, Mater. Res. Bull. 13 (1978) 1447.
- [3] T. Takahashi, H. Iwahara, Esaka, J. Electrochem. Soc. 124 (1977) 1563.
- [4] S.N. Hoda, L.L.Y. Chang, J. Am. Ceram. Soc. 57 (1974) 323.
- [5] B. Begemann, M. Jansen, J. Less-Common Metals 156 (1989) 123.
- [6] D.E. Cox, A.W. Sleight, Solid State Commun. 19 (1976) 969.
- [7] R.J. Kava, B. Batlogg, J.J. Krajewski, R. Farrow, L.W. Ripp Jr., A.E. White, K. Short, W.F. Peck, T. Kometani, Nature 32 (1988) 814.
- [8] N.R. Khasanova, A. Yamamoto, S. Tajima, X.-J. Wu, K. Tanabe, Phys. C 305 (1998) 275.
- [9] N. Kinomura, N. Kumada, Mater. Res. Bull. 30 (1995) 129.
- [10] N. Kumada, N. Kinomura, P.M. Woodward, A.W. Sleight, J. Solid State Chem. 116 (1995) 281.
- [11] N. Kumada, N. Takahashi, N. Kinomura, A.W. Sleight, Mater. Res. Bull. 32 (1997) 1003.
- [12] J. Rodriguez-Carvajal, Phys. B: Condensed Matter. 192 (1993) 55.
- [13] A.I. Vogel, A Text-book of Quantitative Inorganic Analysis, 3rd ed., Longmans, Green & Co., Ltd., London, 1962.
- [14] A.I. Nazza, V.Y. Lee, E.M. Engler, R.D. Jacowitz, Y. Tokura, J.B. Torrance, Phys. C 1367 (1988) 153.
- [15] J.L. Labar, in: L.F. Brno, F. Ciampor (Eds.), Proc. EUREM 12 (2000) 1379.
- [16] H. Mizoguchi, H. Kawazoe, H. Hosono, S. Fujitsu, Solid State Commun. 104 (1997) 705.
- [17] G. Gattow, H. Schroder, Z. Anorg. Chem. 318 (1962) 176.